

LYMPHOID NEOPLASIA

PD-L1 checkpoint blockade prevents immune dysfunction and leukemia development in a mouse model of chronic lymphocytic leukemia

Fabienne McClanahan,^{1,2} Bola Hanna,² Shaun Miller,¹ Andrew James Clear,¹ Peter Lichter,² John G. Gribben,¹ and Martina Seiffert²

¹Centre for Haemato-Oncology, Barts Cancer Institute, London, United Kingdom; and ²Molecular Genetics, German Cancer Research Center, Heidelberg, Germany

Key Points

- In vivo PD-L1 blockade prevents CLL development in the E μ -TCL1 adoptive transfer model.
- In vivo PD-L1 blockade normalizes T-cell and myeloid cell populations and immune effector functions.

Blockade of the programmed cell death 1 (PD-1)/programmed death-ligand 1 (PD-L1) immune checkpoint augments antitumor immunity and induces durable responses in patients with solid cancers, but data on clinical efficacy in leukemias are sparse. Chronic lymphocytic leukemia (CLL) is associated with a tumor-supportive microenvironment and a dysfunctional immune system, as shown by “exhausted” T cells, defective immunologic synapse formation, and immunosuppressive myeloid cells. These defects involve aberrant expression of PD-L1 and are closely mirrored in the E μ -TCL1 mouse model for CLL. In this study, we treated mice after adoptive transfer of E μ -TCL1 CLL with PD-L1–blocking antibodies, which prevented CLL development and was accompanied by a reactivation of immune effector functions. This included restoration of mature macrophages and major histocompatibility complex class II–expressing dendritic cells and prevention of aberrant and exhaustion-like T-cell phenotypes. In addition, PD-L1 blockade restored CD8 T-cell

cytotoxicity and immune synapse formation and normalized T-cell cytokines and proliferation *ex vivo* and *in vivo*. Our data demonstrate that early PD-L1 blockade effectively corrects leukemia-induced immune dysfunction and thus prevents CLL development in mice. Targeting PD-L1/PD-1 interactions should therefore be further explored in clinical studies with CLL patients, ideally in combination with novel compounds to help eliminate CLL. (*Blood*. 2015;126(2):203-211)

Introduction

Immune escape of tumors is a hallmark of carcinogenesis, and restoring antitumor immunity is emerging as a novel treatment approach.¹ Relevant target molecules are immune checkpoints that, under physiological conditions, regulate the activation of immune effector cells to maintain self-tolerance and prevent autoimmunity.² Programmed cell death 1 (PD-1; CD279) and its ligands programmed death-ligand 1 (PD-L1; B7-H1; CD274) and PD-L2 (B7-DC; CD273) constitute one of the most prominent immune checkpoint ligand/receptor axes involved in providing and maintaining an immunosuppressive tumor microenvironment.³ Under physiological conditions, PD-1 is temporarily expressed on immune effector cells upon their activation. Binding of PD-1 by PD-L1 or PD-L2 on antigen-presenting cells results in inhibition of proliferation, cytokine production, and cytotoxic capabilities of T cells. Chronic antigenic stimulation can lead to several progressive phenotypic and functional changes that have been termed “T-cell exhaustion.” These include the hierarchical loss of proliferative capacity and interleukin-2 (IL-2), tumor necrosis factor α (TNF- α), and interferon gamma (IFN- γ) production, which generally coincides with expression of inhibitory surface receptors such as PD-1, LAG-3, CD160, 2B4, TIM-3, and CTLA-4.⁴ Tumors often use aberrant PD-L1 expression to suppress T-cell effector

functions and induce an exhaustion-like state, thereby escaping immune surveillance.³

Chronic lymphocytic leukemia (CLL) is characterized by a clonal expansion of mature B cells that accumulate in peripheral blood (PB), lymphoid organs, and the bone marrow (BM). Several observations support the notion that there is ongoing but insufficient antitumor response in CLL.⁵⁻⁷ Accordingly, various CLL-induced humoral and cellular immune defects contribute to the failure of antitumor immune responses,⁸ and T cells from CLL patients exhibit global molecular defects, which manifest as an impaired ability to form immunologic synapses, aberrant T-cell subsets, and effector function, along with irregular expression of exhaustion-like surface markers such as PD-1.^{6,9-12} Because PD-L1 was shown to be overexpressed on CLL cells and myeloid-derived suppressor cells (MDSCs) from PB of CLL patients,^{10,13} it appears to be an essential mediator of T-cell defects in CLL. These defects and immunosuppressive phenotypes were shown to be recapitulated in E μ -TCL1 mice, a well-characterized transgenic mouse model of CLL, and can be induced in previously healthy mice by adoptive transfer (AT) of murine CLL cells.¹⁴⁻¹⁶

Encouraging results from early clinical trials that used PD-1/PD-L1 antibodies in solid cancers and Hodgkin lymphoma have shown

Submitted January 17, 2015; accepted March 14, 2015. Prepublished online as *Blood* First Edition paper, March 23, 2015; DOI 10.1182/blood-2015-01-622936.

F.M. and B.H. contributed equally to first authorship of this study.

J.G.G. and M.S. contributed equally to last authorship of this study.

The online version of this article contains a data supplement.

There is an Inside *Blood* Commentary on this article in this issue.

The publication costs of this article were defrayed in part by page charge payment. Therefore, and solely to indicate this fact, this article is hereby marked “advertisement” in accordance with 18 USC section 1734.

© 2015 by The American Society of Hematology

significant response rates, thus validating PD-1/PD-L1 as key targets for immunotherapy approaches.^{17,18} Despite the increasing pre-clinical evidence pointing toward the importance of PD-1/PD-L1 inhibitory signaling in CLL, neither PD-1 nor PD-L1 blockade has been clinically explored in this disease. By using E μ -TCL1 mice as a preclinical model for CLL, we hypothesized that *in vivo* PD-L1 blockade would inhibit immune escape, enhance immune responses, and subsequently control disease development.

Materials and methods

Mice, treatment, and sample preparations

All experiments were performed after approval of local animal experimental ethics committees and according to their guidelines. Three-month-old female C57BL/6 wild-type mice (Charles River, Margate, UK) were injected intravenously with 4×10^7 syngeneic splenocytes that were pooled from several leukemic E μ -TCL1 donor mice to ensure an identical composition of donor cells in all recipients. At least 95% of all viable lymphocytes were CD19⁺CD5⁺ CLL cells. Animals were randomized to treatment with 10 mg/kg anti-murine PD-L1 antibody (n = 15; rat immunoglobulin G2b clone 10F.9G2; Bio X Cell, West Lebanon, NH) or rat immunoglobulin G2b κ isotype antibody (n = 10; clone LTF-2; Bio X Cell), both of which are unconjugated and endotoxin-free antibodies tested and validated for usage *in vivo*. On the basis of published reports, antibody administration was started on day +1 and repeated every 3 days by intraperitoneal injection.¹⁹⁻²¹ Mice were euthanized at a predefined end point after 11 doses because previous studies revealed this as an appropriate time point for achieving a fully leukemic state that meets established criteria for CLL in control mice. Matched healthy wild-type (hWT) mice (n = 6) were used as controls. Single-cell suspensions were obtained from PB, BM, peritoneal cavity (PC), and spleen. PB was drawn via cardiac puncture with ethylenediaminetetraacetic acid (EDTA) as an anticoagulant. BM cells were flushed from femurs with 5 mL of phosphate-buffered saline (PBS)/5% fetal calf serum (FCS). Spleen single-cell suspensions were generated by using the gentleMACS tissue dissociator (Miltenyi Biotec, Surrey, UK). Erythrocytes were lysed by using lysis buffer consisting of 154.9 mM NH₄Cl, 10 mM KHCO₃, and 0.1 mM EDTA at pH 7.2. Peritoneal cavity exudates were harvested by injection of 5 to 7 mL of PBS/5% FCS into the PC and subsequent drawing of the PC fluid. Cell counting was performed on an automated Vi-CELL XR hemocytometer (Beckman Coulter, High Wycombe, UK). Spleen sections were embedded in paraffin and stained with hematoxylin and eosin (HE) and antibodies against CD5 and B220. Serum was obtained by centrifugation at 2,000g at 4°C for 20 minutes.

Serum cytokine quantification

Chemokine (C-C motif) ligand 2 (CCL2), interleukin 10 (IL-10), granulocyte-macrophage colony-stimulating factor (GM-CSF), chemokine (C-X-C motif) ligand 2 (CXCL2), chemokine (C-X-C motif) ligand 5 (CXCL5), and TNF- α were measured by MILLIPLEX MAP Mouse Cytokine/Chemokine Magnetic Bead Panel (EMD Millipore, St. Charles, MO) as described by the manufacturer on a Bioplex-200 System (Bio-Rad, Munich, Germany). CCL4, CXCL9 (R&D Systems, Minneapolis, MN) and CXCL16 (RayBiotech, Norcross, GA) were measured by enzyme-linked immunosorbent assay (ELISA) according to manufacturers' protocols.

Flow cytometry

All antibodies used for flow cytometry are listed in supplemental Table 1, available on the *Blood* Web site. Surface staining was performed in PBS/2% FCS/0.02% sodium azide for 30 minutes at 4°C. After washing twice, samples were acquired on a four-laser BD LSRII Fortessa analyzer (BD, Oxford, UK). 4,6-Diamidino-2-phenylindole (DAPI)-negative viable, single mononuclear cells were used for the analysis, and fluorescence-minus-one (FMO) and internal negative controls were always included. FCS files were analyzed by FlowJo software version 7.

Functional assays

Flow cytometry-based functional assays were performed on fresh T cells with or without Phorbol 12-myristate 13-acetate (40.5 μ M)/ionomycin (670 μ M) mitogenic stimulation for 6 hours in the presence of brefeldin A (5.3 mM)/monensin (1 mM; eBioscience, Hatfield, UK) for the last 5 hours. Effector cell activity was assessed by CD107a localization to the surface by adding CD107a-specific antibody to the cells from the beginning of the culture and by detecting intracellular IL-2, IFN- γ , and IL-4 in CD4⁺ and CD8⁺ T cells. Intracellular Ki-67 was determined on unstimulated CD8⁺ T cells. Effector cell function was described as a ratio of CD44⁺CD107a⁺:CD44⁺CD107a⁻ or CD44⁺Ki-67⁺:CD44⁺Ki-67⁻ cells among CD3⁺CD8⁺ cells to depict enrichment (increase of ratio) or loss (decrease of ratio) of effector cells among CD44⁺ populations.

In vivo proliferation

Mice were injected intraperitoneally with 100 μ g per gram of body weight of 5-ethynyl-2'-deoxyuridine (EdU; Life Technologies, Paisley, UK) 20 hours before they were euthanized. A total of 2×10^6 splenocytes were prepared for EdU detection by Alexa Fluor 488 dye following the manufacturer's instructions and stained for CD5, CD19, CD8, CD11b, and CD11c. Analysis was performed on single mononuclear cells, and proliferating cells were identified as Alexa488-positive populations on the basis of negative internal controls without Alexa488 in the EdU reaction cocktail.

Immune synapse assay

Frozen splenocytes were debulked from CLL or B cells by magnetic isolation using murine CD19 microbeads (Miltenyi Biotec). The column effluent representing the CD19⁻ fraction was further purified by negative selection using the murine pan T-cell isolation kit (Miltenyi Biotec). Synapse assays and confocal microscopy were performed as previously described.⁹ Briefly, 7-amino-4-chloromethylcoumarin-labeled (CMAC), staphylococcal enterotoxin A and B (SEA/SEB) (2 μ g/mL; Sigma-Aldrich, Gillingham, UK) superantigen-pulsed healthy syngeneic B cells were used as antigen-presenting cells at a 1:1 ratio with T cells from anti-PD-L1 (aPD-L1) and isotype-treated and hWT mice. The AxioVision outline tool (Zeiss, Cambridge, UK) was used to mark each synapse between T and B cells, and all available interactions were scored in each condition. The synapse area was reported as the area of T-cell F-actin immune synapses (μ m²) value.

Statistical considerations

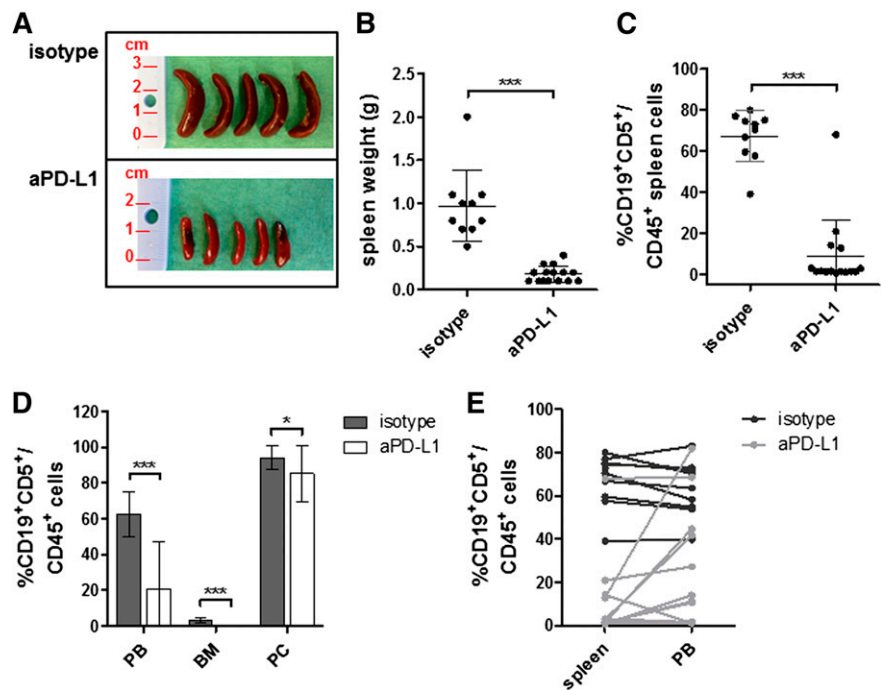
Mouse sample size calculations were based on the assumption that at least 9 mice per group would be needed to detect a 1.25 standard deviation (SD) difference between treated and untreated mice in one-sided testing at a significance level $\alpha = .05$ with at least 80% power. All data sets were tested for normality by using the Shapiro-Wilk test. For normally distributed data sets, an unpaired Student *t* test was used to analyze differences between groups; for non-normally distributed data sets, the two-sided Mann-Whitney *U* test was used. *P* values of less than .05 were considered statistically significant. Analyses were conducted by using Prism Version 5 software (GraphPad). Values are reported as median \pm SD, unless indicated otherwise.

Results

Anti-PD-L1 treatment effectively controls CLL development in mice after AT

To test our hypothesis on the role of PD-L1 in CLL development, we treated mice after AT of 4×10^7 CLL cells from leukemic E μ -TCL1 donor animals with aPD-L1 or isotype control antibody (see "Mice, treatment, and sample preparations" in "Materials and methods" for the detailed treatment regimen). Treatment with aPD-L1 resulted in effective control of CLL development with remarkably reduced spleen sizes compared with isotype antibody-treated mice (Figure 1A)

Figure 1. In vivo anti-PD-L1 treatment effectively controls CLL development after AT. Three-month-old C57BL/6 healthy hWT mice transplanted with 4×10^7 CLL cells from leukemic E μ -TCL1 mice were randomized to treatment with 10 mg/kg rat immunoglobulin G2b (IgG2b) aPD-L1 (n = 15) or rat IgG2bk isotype antibody (n = 10) administered intraperitoneally every 3 days starting 1 day after AT and were euthanized 31 days later. (A) Differences in spleen sizes between isotype and anti-PD-L1-treated mice. (B) Compared with isotype-treated controls, median spleen weights (g) of aPD-L1-treated mice were significantly reduced. (C-D) Single-cell suspensions of CLL-affected organs were analyzed by flow cytometry, and cells were gated on total viable 4,6 diamidino-2-phenylindole (DAPI)-negative single CD45⁺ cells. Tumor load, defined as percentage of CD5⁺CD19⁺ cells of total CD45⁺ hematopoietic cells, in (C) spleen and (D) PB, BM, and PC was compared between isotype- and aPD-L1-treated mice. (E) Tumor load distribution in spleen and PB depicted for individual mice, suggesting more effective disease control in secondary lymphoid organs than in PB. All graphs depict mean \pm SD. **P* < .05; ****P* < .0001.



and significantly lower median spleen weights (0.2 g vs 0.9 g; *P* < .0001; Figure 1B). Quantification of tumor loads in affected tissues revealed a significantly lower median relative frequency of CD19⁺CD5⁺ CLL lymphocytes in spleen as the representative organ of involved secondary lymphoid tissues (1.55% vs 71.69%; *P* < .0001; Figure 1C), in PB (10.50% vs 63.53%; *P* = .0019), in BM (0.26% vs 2.74%; *P* < .0001), and to a lesser degree in the PC (92.36% vs 96.84%; *P* = .0315) of aPD-L1-treated mice compared with isotype controls (Figure 1D and supplemental Figure 1), indicating effective tumor control. Lymph nodes, the primary site of disease in humans, are barely affected in the E μ -TCL1 AT mouse model when the transplantation regimen routinely applied by our group was used; therefore they were not included. No significant weight loss (22.27 ± 0.37 g vs 22.50 ± 0.45 g mean weight of aPD-L1 vs hWT mice) or signs of sickness were observed at the end point in antibody-treated mice. Despite being clearly less affected by disease, aPD-L1-treated mice still showed histologic evidence of disrupted spleen architecture by infiltrating CD5⁺B220⁺ lymphocytes, indicating successful homing and engraftment of CLL cells (supplemental Figure 2). Interestingly, clearance of CLL cells appeared more effective in spleen than in PB in the majority of mice (Figure 1E), suggesting either an effect on migration or homing of CLL cells or a tissue-specific control mechanism of aPD-L1. Although PD-L1 expression could not be determined in aPD-L1-treated mice because of steric hindrance of binding of clone MIH5 detection antibodies,²² PD-L1 overexpression was confirmed on CLL cells as well as on monocytes and dendritic cells in leukemic mice treated with isotype antibody compared with hWT controls (supplemental Figure 3). Collectively, our data show that PD-L1 blockade very effectively controls CLL development in the AT model.

PD-L1 blockade resolves systemic inflammation, repairs CLL-associated myeloid cell skewing, and improves dendritic cell maturation

To test whether PD-L1 blockade affects the immune status in treated mice, we first quantified inflammatory serum factors in mice after AT of CLL cells (Figure 2A). CCL4, a cytokine that is known to be released

by stimulated CLL cells,²³ was significantly lower in aPD-L1-treated mice. In addition, several inflammatory cytokines, including TNF- α , granulocyte-macrophage colony-stimulating factor, CXCL2, and CXCL5, as well as the T-cell chemoattractants CXCL9 and CXCL16 normalized to hWT levels after treatment. Importantly, the immunosuppressive cytokine IL-10 decreased considerably in aPD-L1-treated mice. A summary of cytokine/chemokine serum level data is provided in supplemental Table 2.

Because the serum levels of CCL2, a chemoattractant for monocytes, also decreased in aPD-L1-treated mice, we used flow cytometry to investigate whether treatment had an impact on myeloid cell infiltration and subset composition. Splenic monocytes were defined as Lin⁻ (CD19, CD3, Ly6G, and NK1.1) CD11b⁺F4/80^{int}CD11c^{low-int}MHC-II^{low}SSC^{int} cells as previously described.²⁴ We observed a decrease of relative monocyte percentage in the spleens of mice treated with aPD-L1 to $1.16\% \pm 0.27\%$ of the non-B-cell fraction compared with $6.13\% \pm 0.81\%$ in isotype-treated controls (*P* < .0001; Figure 2B). Increased numbers of nonclassical monocytes with high CD16 expression were described in PB of CLL patients.²⁵ These so-called patrolling monocytes play a key role in monitoring endothelial integrity and tissue regeneration after inflammation. Because we have confirmed a severe skewing of monocytes toward patrolling phenotype in leukemic E μ -TCL1 mice (B.H., F.M., Nadja Zaborsky, Claudia Dürr, Axel Benner, Verena Kalter, Alexander Egle, J.G.G., P.L., and M.S., manuscript submitted), we determined the composition of splenic monocytes in aPD-L1- and isotype-treated mice by using Ly6C and CD43 to differentiate between inflammatory (Ly6C^{hi}CD43^{low}), intermediate (Ly6C^{hi}CD43^{hi}), and patrolling (Ly6C^{low}CD43^{hi}) monocyte subsets (Figure 2C, left) as previously described.²⁶ Treatment with aPD-L1 resulted in significantly lower percentages of patrolling monocytes compared with isotype-treated controls ($22.95\% \pm 2.12\%$ vs $49.93\% \pm 4.71\%$; *P* < .0001) and increased percentages of intermediate monocytes (Figure 2C, right). Because patrolling monocytes represent a later differentiation state of inflammatory monocytes,^{27,28} the increased percentage of intermediate monocytes after aPD-L1 treatment might imply a step-wise

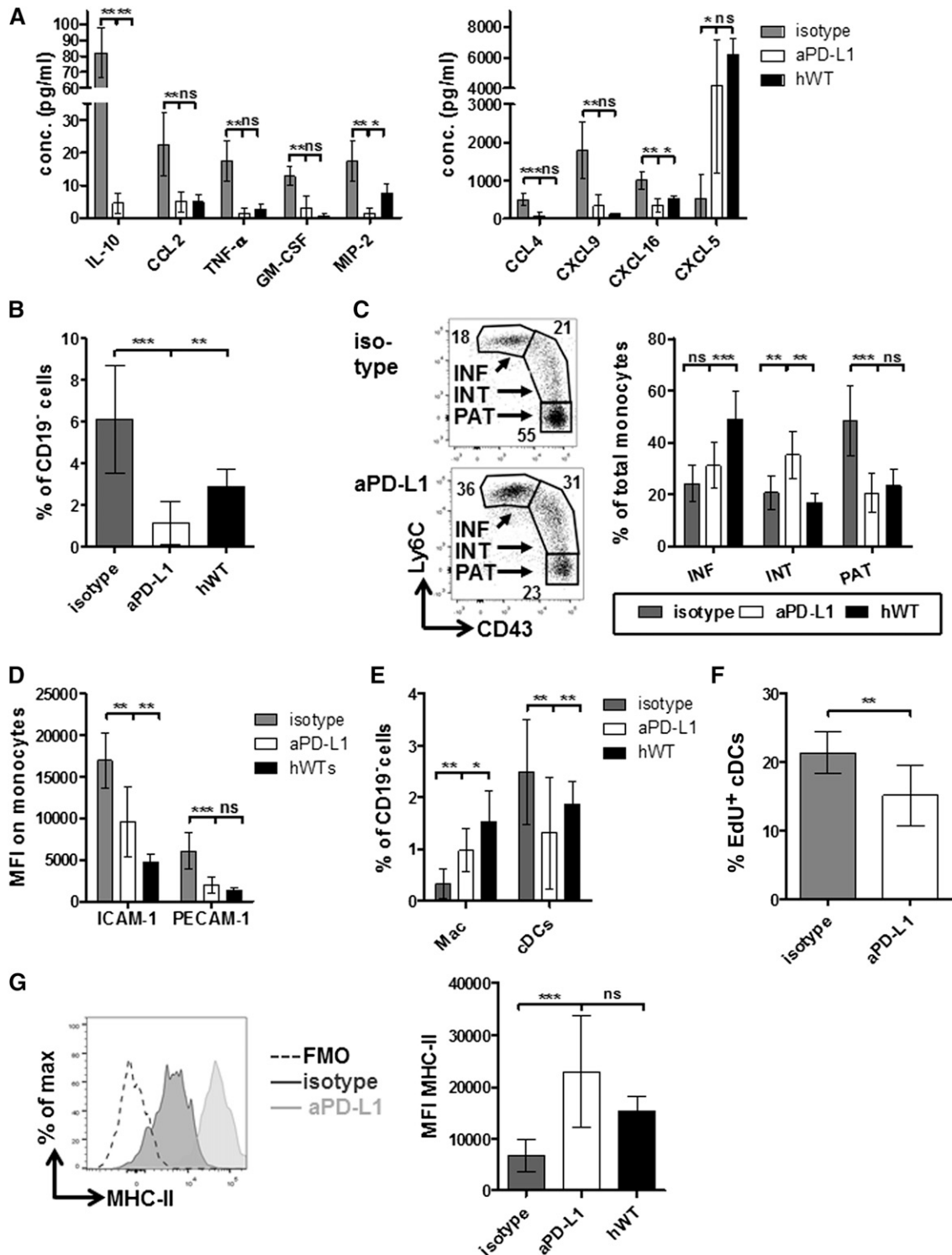


Figure 2. In vivo anti-PD-L1 treatment resolves systemic inflammation and repairs CLL-induced myeloid skewing. (A) Blood was collected by cardiac puncture, and serum levels (pg/mL) of IL-10, CCL2, TNF- α , granulocyte-macrophage colony-stimulating factor, MIP-2 (CXCL2), CCL4, CXCL9, CXCL16, and CXCL5 were analyzed in isotype ($n = 5$), aPD-L1 ($n = 7$), and hWT ($n = 5$) mice using multiplex bead arrays or enzyme-linked immunosorbent assay. (B) Spleen single-cell suspensions were analyzed by flow cytometry. Monocytes were defined as Lin⁻(CD19, CD3, Ly6G, and NK1.1)CD11b⁺F4/80^{int}CD11c^{low-int}MHC-II^{low}SSC^{int} cells, and their percentages of total viable spleen CD19⁻ mononuclear cells (MNCs) were compared between isotype ($n = 9$), aPD-L1 ($n = 14$), and hWT ($n = 5$) mice. (C) Spleen monocyte subsets were defined on the basis of expression of Ly6C and CD43 as inflammatory (INF; Ly6C^{hi}CD43^{low}), intermediate (INT; Ly6C^{hi}CD43^{hi}), and patrolling (PAT; Ly6C^{low}CD43^{hi}) monocytes. A representative example of the gating is depicted (left panel, numbers indicate percentage of populations), and a quantification after gating on total monocytes of at least 9 animals per group are shown (right panel). (D) Expression of adhesion molecules PECAM-1 and ICAM-1 was analyzed in splenic monocytes, and mean fluorescence intensities (MFIs) were compared. (E) Percentage of macrophages, defined as Lin⁻CD11b^{low}F4/80^{hi} cells, and conventional dendritic cells (cDCs), defined as CD11c^{hi}CD11b⁺ cells, of CD19⁺ cells in spleens were compared. (F) In vivo proliferation of cDCs (CD11c^{hi}CD11b⁺) in spleen was assessed as percentage of EduU-positive cells of at least 10 mice per group injected with 100 μ g per gram body weight before being euthanized. (G) MHC-II expression was analyzed on splenic CD11c^{hi}CD11b⁺ cDCs. A representative histogram is depicted (left panel), and MFIs of at least 9 mice per group are shown (right panel). All graphs depict mean \pm SD. FMO, fluorescence-minus-one; Mac, macrophage; ns, not significant; * $P < .05$; ** $P < .001$; *** $P < .0001$.

repair of monocyte skewing. Accordingly, aPD-L1 blockade decreased the expression of adhesion molecules ICAM1 and PECAM1 on monocytes, which are known to be highly expressed on patrolling monocytes, confirming the reversal of CLL-induced monocyte skewing (Figure 2D and supplemental Figure 4).

CLL development is associated with changes within myeloid cell subsets and their activity, which includes an aberrantly high expression of PD-L1 on myeloid cells.^{13,23} Because the presence of aPD-L1-blocking antibodies in the treated animals prevented detection of PD-L1 by flow cytometry, PD-L1 expression levels on myeloid cells upon treatment could not be captured. In leukemic mice, splenic macrophages defined as Lin⁻CD11b^{low}F4/80^{hi} cells were dramatically decreased, which was reversed after PD-L1 blockade, resulting in a higher percentage of non-B cells compared with the control group (0.97% ± 0.11% vs 0.32% ± 0.09%; *P* < .001; Figure 2E). Conversely, conventional dendritic cells (cDCs), defined as CD11c^{hi}CD11b⁺ cells, represented a lower percentage of non-B cells in aPD-L1-treated mice compared with controls (1.32% ± 0.28% vs 2.49% ± 0.32%; *P* = .0054; Figure 2E). This was supported by in vivo EdU incorporation assays, in which a lower percentage of EdU-positive cDCs was detected in aPD-L1-treated mice compared with isotype controls (15.17% ± 1.24% vs 21.41% ± 0.94%; *P* = .001; Figure 2F). Interestingly, cDCs showed a higher expression of major histocompatibility complex class II (MHC-II) molecules upon PD-L1 blockade, suggesting an increased antigen-presenting capacity in comparison with isotype controls (Figure 2G). Collectively, our data show that PD-L1 blockade reverses CLL-induced skewing of myeloid cells and promotes their differentiation toward macrophages or mature MHC-II^{high} DCs.

PD-L1 blockade corrects CLL-induced aberrant T-cell phenotype and improves activation status of T cells

In addition to restoring cell subsets and phenotypes in the myeloid compartment, in vivo aPD-L1 led to significant corrections of T-cell phenotypes: although isotype-treated mice exhibited typical CLL-induced broad phenotypic T-cell defects (namely, a relative loss of CD3⁺ cells, and among CD3⁺ cells, a relative loss of CD4⁺ and a relative increase of CD8⁺ cells), the relative median frequencies of CD3⁺, CD3⁺CD4⁺, and CD3⁺CD8⁺ T cells were restored by aPD-L1 treatment to levels observed in hWT mice (Figure 3A), resulting in a normalization of the CD4:CD8 ratio in spleen (1.60 ± 0.24 vs 0.65 ± 0.16; *P* < .0001), BM (0.39 ± 0.09 vs 0.24 ± 0.02; *P* = .0002), and PB (1.51 ± 0.81 vs 0.37 ± 0.42; *P* < .0001) (Figure 3B). Among splenic CD3⁺CD8⁺ T cells, the loss of naïve CD44⁻ cells and shift to antigen-experienced CD44⁺ cells with a relative expansion of CD62L⁻CD44⁺ effector and CD62L⁻CCR7⁻ effector memory cells was significantly reduced by aPD-L1 treatment (Figure 3C; means ± SD and *P* values are summarized in supplemental Table 3; gating strategy is shown in supplemental Figure 5A). Very similar effects were observed in PB and BM, indicating a systemic repair of CLL-driven T-cell subset alterations in different sites of the lymphoid system (supplemental Figure 5B-E). In addition, the expression of previously described surface exhaustion markers PD-1 (9.86% ± 4.24% vs 19.42% ± 5.81%), KLRG-1 (6.55% ± 3.75% vs 33.71% ± 10.78%), 2B4 (1.81% ± 1.26% vs 31.13% ± 28.92%), and LAG3 (1.49% ± 1.30% vs 7.67% ± 2.31%), but not CD160 (4.97% ± 1.44% vs 5.14% ± 0.97%), were significantly reduced in aPD-L1-treated compared with isotype-treated mice (Figure 3D). Reduced PD-1 expression was also recapitulated in CD3⁺CD8⁺ cells in BM and PB (supplemental Figure 5F). However, PD-1 expression in cells from aPD-L1-treated mice was still increased

compared with hWT mice, highlighting the activation status of T cells during the anti-CLL immune response. Among CD3⁺CD4⁺ cells from spleen, similar repair effects of T-cell subsets and PD-1 expression were observed (Figure 3E, supplemental Table 3). In sum, our findings indicate that early in vivo PD-L1 blockade corrects CLL-induced aberrant CD3⁺CD8⁺ and CD3⁺CD4⁺ T-cell subset distributions and reduces the expression of typical exhaustion markers regardless of the microenvironment, and that cells show phenotypic signs of activation.

Anti-PD-L1 treatment corrects T-cell effector functions essential for antitumor immune response

After confirming that aPD-L1 treatment corrects the development of typical CLL-induced T-cell phenotype defects, we examined the ability to repair T-cell effector function in cells from spleen. In antigen-experienced CD44⁺CD3⁺CD4⁺ T cells, aPD-L1 treatment significantly reduced the typical CLL-induced relative loss of IL-2 expression (5.05% ± 0.82% vs 3.26% ± 1.88%; *P* = .0043) and the increase of IL-4 (5.55% ± 2.49% vs 10.13% ± 2.23%; *P* = .0004) and IFN-γ-expressing cells (6.96% ± 3.08% vs 9.54% ± 2.16%; *P* = .0247; Figure 4A) after mitogenic stimulation, suggesting a correction of aberrant stereotypical Th1/Th2 cytokines. However, this was still markedly different compared with hWT mice, indicating an antitumor cytokine reaction. In CD8⁺ T cells, aPD-L1 prevented the loss of antigen-experienced CD44⁺CD3⁺CD8⁺ cells with the ability to localize lysosomal CD107a to their surface upon mitogenic stimulation (CD107a ratios 3.12 ± 1.38 vs 1.76 ± 0.42; *P* < .0001; Figure 4B), which is indicative of restored effector cell cytotoxicity. This was supported by the observation that aPD-L1 treatment restored the ability of autologous T cells to form immunologic synapses with healthy B cells as antigen-presenting cells (2.47 ± 0.87 μm² vs 1.47 ± 0.49 μm²; *P* < .0001; Figure 4C), probably as a result of reduced PD-1 expression that affects immune synapse modeling. In addition, aPD-L1 treatment corrected aberrant CLL-induced T-cell proliferation: both the increased Ki-67 ratio in CD44⁺CD3⁺CD8⁺ cells, indicative for an enrichment of proliferating antigen-experienced cells (0.13 ± 0.06 vs 0.47 ± 0.13; *P* < .0001; Figure 4D), and the percentages of Alexa Fluor 488-labeled EdU⁺CD4⁺ (2.13% ± 2.00% vs 11.50% ± 2.47%; *P* < .0001) and EdU⁺CD8⁺ T cells (1.19% ± 1.22% vs 2.70% ± 0.85%; *P* = .0213; Figure 4E) were significantly reduced in aPD-L1-treated mice. Our findings on CLL-induced increased T-cell proliferation in mice are in contrast to that in human T cells, in which decreased proliferation has been described in the context of CLL.⁶ This is most likely related to the different organs T cells were taken from: whereas human T-cell proliferation was determined in PB, murine proliferation was assessed in T cells from spleen, in which the microenvironment is likely to provide different proliferation stimuli.²⁹ Taken together, our functional data indicate that in vivo anti-PD-L1 treatment corrects the development of typical previously described CLL-induced effector T-cell defects and partly restores effector function to normal levels observed in hWT mice, but signs of functional activation as a result of ongoing antitumor responses are present.

Discussion

Our current understanding of the immune system in CLL suggests that there are ongoing but highly ineffective antitumor responses. The expansion of CD8⁺ T cells, their skewing toward effector and

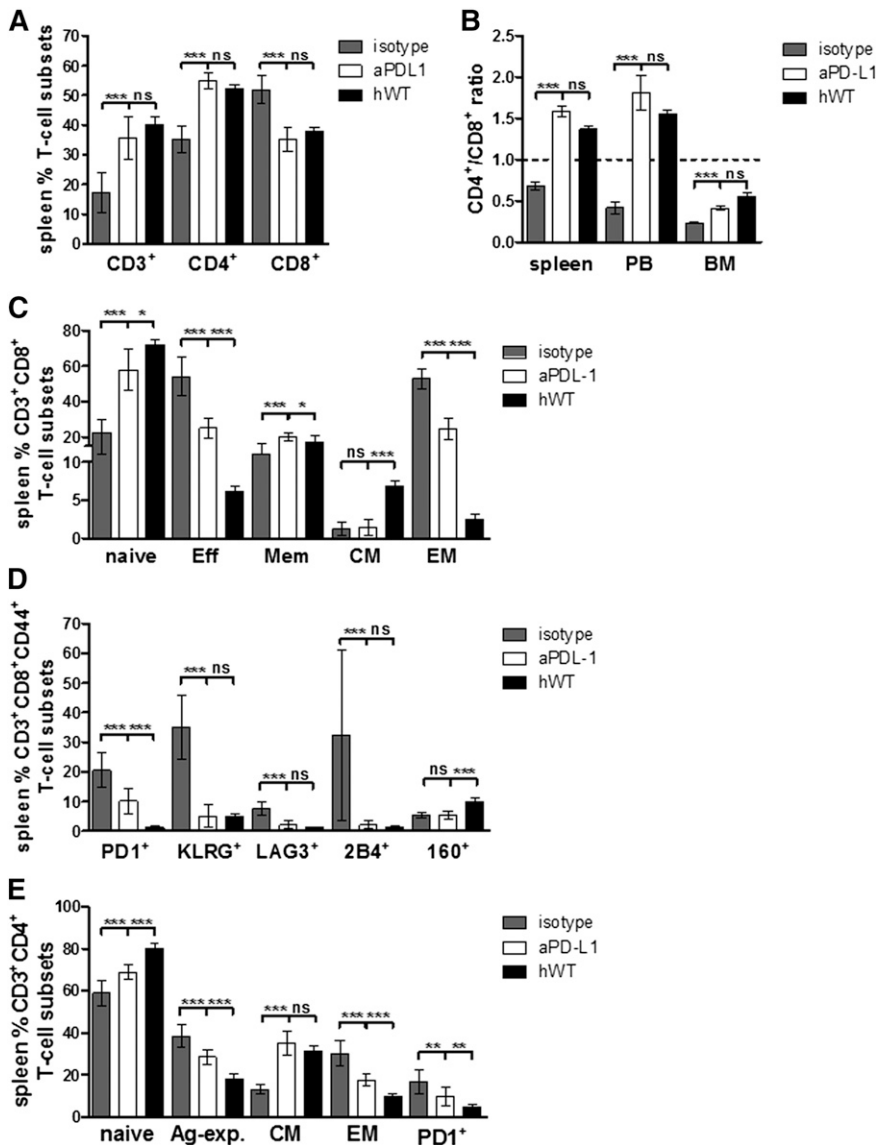


Figure 3. In vivo anti-PD-L1 treatment prevents development of typical CLL-induced aberrant T-cell phenotype. Fresh cells of isotype ($n = 10$), aPD-L1-treated ($n = 15$), and hWT ($n = 6$) mice were stained for CD3, CD4, CD8, CD44, CCR7, and CD62L, and T cells were gated on DAPI-negative, viable, single MNCs. (A) CD3⁺ T cells from spleen, depicted as percentage of all lymphocytes, as well as CD4⁺ and CD8⁺ T cells, depicted as percentage of all CD3⁺ T cells, were compared. (B) CD4⁺:CD8⁺ ratios among CD3⁺ T cells were calculated for cells in spleen, PB, and BM and compared between isotype, aPD-L1, and hWT mice. (C) Naive (CD44⁺CD62L⁻), effector (Eff; CD44⁺CD62L⁻), memory (Mem; CD44⁺CD62L⁺), effector memory (EM; CD44⁺CD62L⁺CCR7⁺), and central memory (CM; CD44⁺CD62L⁺CCR7⁻) T cells were quantified and are presented as percentage of CD3⁺CD8⁺ cells in spleen. (D) The percentages of antigen-experienced (Ag-exp.) CD44⁺CD3⁺CD8⁺ T cells expressing exhaustion markers PD-1, KLRG-1, 2B4, LAG3, and CD160 were quantified in spleen. (E) Naive (CD44⁺CD62L⁻), Ag-exp. CD44⁺, EM (CD44⁺CD62L⁺CCR7⁺), and CM (CD44⁺CD62L⁺CCR7⁻) CD3⁺CD4⁺ T cells and the percentage of Ag-exp. CD44⁺CD3⁺CD4⁺ T cells expressing PD-1 were quantified in spleen. All graphs depict mean \pm SD. * $P < .05$; ** $P < .001$; *** $P < .0001$.

terminally differentiated T cells, the relatively limited T-cell receptor repertoire, and enhanced secretion of inflammatory cytokines such as IFN- γ and TNF- α support the notion that immune reactions are present in CLL.^{6,16} However, this chronic antigenic stimulation of the immune system leads to a constant presence of defective effector cells and provides an inflammatory milieu. Moreover, CLL cells develop adaptive resistance mechanisms to alter and escape from endogenous antitumor immune responses, and immune checkpoint ligands such as PD-L1 play a key role in this. Interestingly, inflammatory cytokines such as IFN- γ have been demonstrated to induce PD-L1 expression on both tumor and myeloid cells in the microenvironment,³⁰⁻³² which might define a central event in switching the immune system to a permissive tumor-friendly state. By using the well-established E μ -TCL1 mouse model of CLL, we found that blocking PD-L1 in vivo during CLL engraftment may reactivate the immune system by counteracting CLL-induced defects in myeloid and T-cell populations. As a result of successful PD-L1 blockade, CD4⁺ and CD8⁺ effector T-cell functions essential for antitumor immune responses such as cytotoxicity, cytokine production, and immune synapse formation were improved, which in turn led to

further disease control. Consequently, further immune defects induced by chronic antigenic stimulation were resolved as shown by the repair of skewed CD4:CD8 ratios, correction of lost naïve and enriched antigen-experienced CD4⁺ and CD8⁺ T cells that express markers of exhaustion, and control of T-cell proliferation. In addition, in vivo aPD-L1 blockade abrogated the CLL-induced differentiation blockade of myeloid cells, indicated by an increased number of macrophages in the spleen, higher MHC-II levels on dendritic cells, and the disappearance of patrolling monocytes. In total, CLL-associated chronic inflammation was resolved as shown by normalized cytokine/chemokine serum levels. We observed, in association with reactivated immune functions, control of CLL development by PD-L1 blockade, which led to a significant reduction of tumor load in disease-affected tissues. Whereas this effect was very pronounced in blood, BM, and spleen, only a minor reduction in CLL cell counts was observed in PC, suggesting either an effect on migration or homing of CLL cells or a tissue-specific control mechanism of aPD-L1. CLL cells that have infiltrated the PC might not be controlled by PD-L1/PD-1 interactions, and other immune checkpoint axes such as PD-L2/PD-1 might be of relevance.³ Because involvement

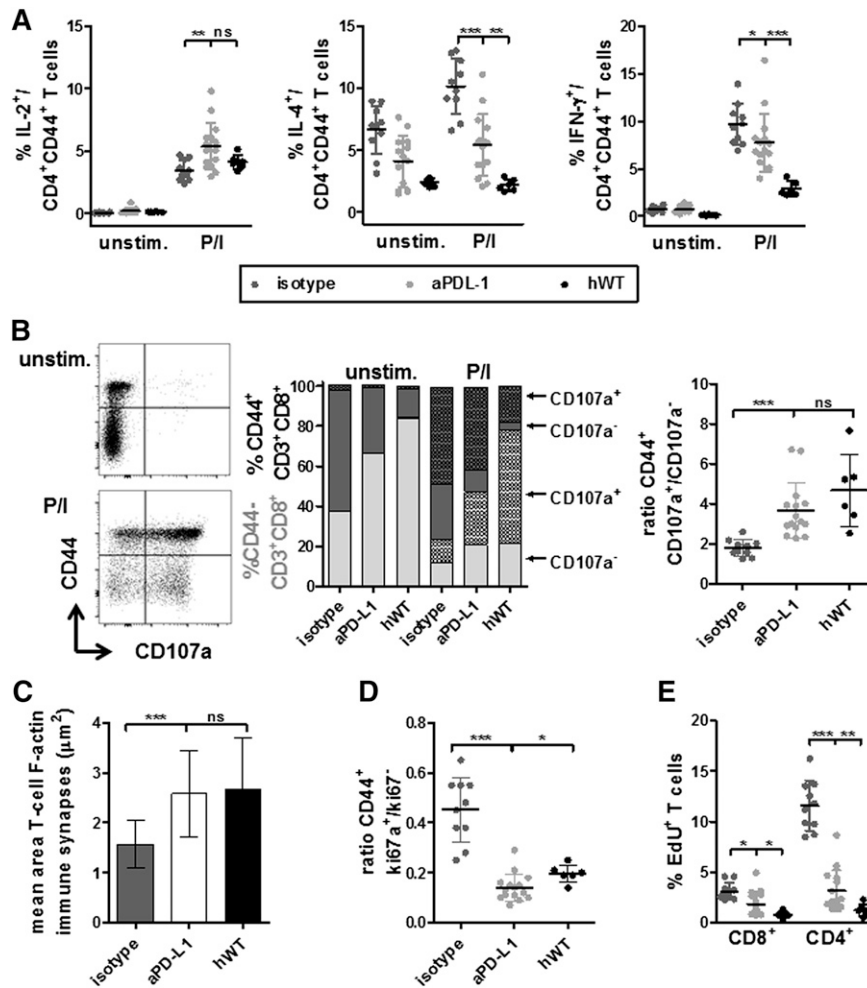


Figure 4. In vivo anti-PD-L1 treatment restores key T-cell effector functions. Fresh splenocytes of isotype (n = 10), aPD-L1-treated (n = 15), and hWT (n = 6) mice were cultured for 6 hours with or without phorbol myristate acetate (PMA)/ionomycin (P/I) in the presence of brefeldin A/monensin during the last 5 hours. (A) After surface staining for CD3, CD4, CD8, and CD44 and permeabilization/fixation, cells were stained for intracytoplasmic IL-2, IL-4, and IFN-γ-positive cells of CD44⁺ CD3⁺ CD8⁺ viable, single MNCs were calculated. Unstimulated cells (unstim.) and FMO controls were included in the analysis, and percentages of IL-2, IL-4, and IFN-γ-positive cells of CD44⁺ CD3⁺ CD8⁺ T cells were calculated. (B) Effector cell cytotoxicity was assessed by CD107a localization to the cell surface upon mitogenic stimulation with P/I. CD107a antibody was added from the beginning of the 6-hour in vitro culture period. Naïve and Ag-exp. CD3⁺ CD8⁺ cytotoxic effector T-cell subsets were discriminated by expression of CD44. Unstimulated cells were used as controls. Left panel: representative flow cytometry dot plots. Center panel: quantification of CD107a-expressing cells within CD44⁺ naïve (light gray) and CD44⁺ Ag-exp. cells (dark gray). Right panel: because of different relative frequencies of CD44⁺ cells between experimental groups, T-cell function was compared by calculating ratios of CD44⁺ CD107a⁺:CD44⁺ CD107a⁻ cells of all CD3⁺ CD8⁺ T cells to describe enrichment (increased ratio) or loss (decreased ratio) of effector cells within the CD44⁺ population. (C) Splenic T cells taken from aPD-L1, isotype, and hWT mice were mixed with 7-amino-4-chloromethylcoumarin-labeled, superantigen-pulsed healthy syngeneic B cells as antigen-presenting cells at a 1:1 ratio, centrifuged onto poly-lysine-coated microscope slides, and F-actin was stained with rhodamine-phalloidin. Immune synapse formation between T and B cells was quantified by confocal laser-scanning microscopy using AxioVision image analysis software. The synapse area is depicted as mean area of T-cell F-actin immune synapses (μm²) value. (D) To assess ex vivo proliferation of unstimulated cytotoxic T cells, intranuclear Ki-67 staining was analyzed by flow cytometry based on FMO controls and is given as a ratio among CD44⁺ cells as described in (B). (E) In vivo proliferation of CD8⁺ and CD4⁺ T cells in spleen was assessed after injection with 100 μg per gram body weight EdU 20 hours before being euthanized as a percentage of EdU⁺ cells after gating on single CD5⁺ T cells. All graphs depict mean ± SD. *P < .05; **P < .001; ***P < .0001.

of the PC is not described or routinely tested in human CLL, these findings in mice are of only minor relevance for clinical applications of PD-L1 blockade. Nevertheless, they clearly exclude a direct cytotoxic effect of the antibody for PD-L1-expressing CLL or myeloid cells, which is in line with the absence of data describing direct cytotoxic activity or antibody-dependent cellular cytotoxicity for this antibody.¹⁹⁻²¹ Instead, it seems feasible that effective tumor control resulted from a restoration of immune effector functions by continuous anti-PD-L1 blockade, which prevented the induction of immune tolerance in secondary lymphoid organs, where interactions between PD-L1-expressing myeloid and CLL cells and PD-1-expressing T cells mostly occur.

Although our previous in vitro work using coculture systems of CLL and T cells clearly demonstrated that global T-cell defects and PD-L1-mediated impaired T-cell function were induced by direct cell-cell contact with malignant CLL cells,^{9,10,33} several studies have

now demonstrated that aberrant PD-L1 expression by MDSCs and tumor-associated macrophages in the tumor microenvironment also exert an inhibitory effect on T-cell function, partly via PD-L1/PD-1 inhibitory signaling.^{34,35} That is why it is most likely that PD-1/PD-L1 interactions are of importance in T-cell/CLL cell as well as T-cell/myeloid cell communication. To fully understand the complexity of this cross-talk and its contribution to disease development and progression, it is important to further characterize the interactions between T cells and tumor-associated macrophages and/or MDSCs in vivo, to identify the stages of disease development during which they occur and what the underlying mechanisms are.

Because our findings highlight the importance of the PD-L1/PD-1 checkpoint in initiating and maintaining immunosuppressive activity in CLL, they indicate that success of treatment with aPD-L1 is the result of a reactivation of antitumor immunity. This is in

concordance with published data from murine solid cancer models, which indicate that in vivo PD-L1 blockade in combination with IL-15 administration, CTLA-4 blockade, or indoleamine 2,3-dioxygenase pathway blockade restores CD8⁺ T-cell IL-2 production and proliferation within the tumor microenvironment,³⁶ increases the number of and lytic activity of tumor antigen-specific CD8⁺ T cells, and inhibits suppressive functions of regulatory T cells.^{37,38} We observed that CLL development in E μ -TCL1 mice is associated with increased numbers of immature myeloid cells with aberrantly upregulated PD-L1 expression (B.H., F.M., Nadja Zaborsky, Claudia Dürr, Axel Benner, Verena Kalter, Alexander Egle, J.G.G., P.L., and M.S., manuscript submitted), mirroring findings in human CLL.¹³ We anticipate that CLL cells evade T-cell immunity by inducing immunosuppressive and tolerogenic effector cell phenotypes and that this contributes to disease progression, similar to reports in other entities.^{34,39}

Clinical data on aPD-L1 antibodies in patients with leukemia or lymphomas is scant. Immune checkpoint blockade by the PD-1-specific antibody pidilizumab showed a favorable safety profile and evidence of clinical activity in patients with hematologic malignancies, including a small number of CLL cases.⁴⁰ Of interest, changes within circulating lymphocyte subsets during treatment suggested an activation of antitumor immune responses. In another study, pidilizumab was combined with the anti-CD20 antibody rituximab and showed activity in patients with relapsed follicular lymphoma.⁴¹ This was associated with an increase in CD3⁺CD4⁺ T cells, and response to treatment correlated with a T-cell activation signature. A recent study using the PD-1-specific antibody nivolumab showed a favorable safety profile and substantial therapeutic activity in patients with previously treated relapsed or refractory Hodgkin lymphoma.¹⁸

In summary, our in vivo data derived from the E μ -TCL1 mouse model provide a strong rationale for further clinical assessment of PD-1/PD-L1 immune checkpoint blockade in CLL. An attractive

approach would be to use checkpoint inhibition in combination with agents targeting B-cell receptor signaling. Here, treatment with B-cell receptor inhibitors would mobilize and decrease the tumor bulk, whereas eradication of residual disease and durable remissions could be achieved by the reactivation and restoration of antitumor immune responses by PD-1/PD-L1 blockade.

Acknowledgments

This work was supported by the Helmholtz Virtual Institute “Understanding and Overcoming Resistance to Apoptosis and Therapy in Leukemia,” by grants from the National Institutes of Health to the Chronic Lymphocytic Leukemia Research Consortium, and by grant P01 CA95426 from the National Cancer Institute (J.G.G.).

Authorship

Contribution: F.M. and B.H. designed the study, acquired, analyzed, and interpreted data, prepared figures, wrote the manuscript, and contributed equally to the study as first authors; S.M. and A.J.C. acquired data; P.L. supervised the study and reviewed the manuscript; and J.G.G. and M.S. designed and supervised the study, interpreted data, wrote the manuscript, and contributed equally to the study as last authors.

Conflict-of-interest disclosure: The authors declare no competing financial interests.

Correspondence: Martina Seiffert, German Cancer Research Center, Im Neuenheimer Feld 280, Heidelberg, 69120, Germany; e-mail: m.seiffert@dkfz.de.

References

- Schreiber RD, Old LJ, Smyth MJ. Cancer immunoeediting: integrating immunity's roles in cancer suppression and promotion. *Science*. 2011;331(6024):1565-1570.
- Pardoll DM. The blockade of immune checkpoints in cancer immunotherapy. *Nat Rev Cancer*. 2012;12(4):252-264.
- Greaves P, Gribben JG. The role of B7 family molecules in hematologic malignancy. *Blood*. 2013;121(5):734-744.
- Wherry EJ. T cell exhaustion. *Nat Immunol*. 2011;12(6):492-499.
- Burkhardt UE, Hainz U, Stevenson K, et al. Autologous CLL cell vaccination early after transplant induces leukemia-specific T cells. *J Clin Invest*. 2013;123(9):3756-3765.
- Riches JC, Davies JK, McClanahan F, et al. T cells from CLL patients exhibit features of T-cell exhaustion but retain capacity for cytokine production. *Blood*. 2013;121(9):1612-1621.
- Rezvan M-R, Jeddi-Tehrani M, Wiggall H, Österborg A, Mellstedt H. Leukemia-associated monoclonal and oligoclonal TCR-BV use in patients with B-cell chronic lymphocytic leukemia. *Blood*. 2003;101(3):1063-1070.
- Riches JC, Gribben JG. Understanding the immunodeficiency in chronic lymphocytic leukemia: potential clinical implications. *Hematol Oncol Clin North Am*. 2013;27(2):207-235.
- Ramsay AG, Johnson AJ, Lee AM, et al. Chronic lymphocytic leukemia T cells show impaired immunological synapse formation that can be reversed with an immunomodulating drug. *J Clin Invest*. 2008;118(7):2427-2437.
- Ramsay AG, Clear AJ, Fatah R, Gribben JG. Multiple inhibitory ligands induce impaired T-cell immunologic synapse function in chronic lymphocytic leukemia that can be blocked with lenalidomide: establishing a reversible immune evasion mechanism in human cancer. *Blood*. 2012;120(7):1412-1421.
- Brusa D, Serra S, Coscia M, et al. The PD-1/PD-L1 axis contributes to T-cell dysfunction in chronic lymphocytic leukemia. *Haematologica*. 2013;98(6):953-963.
- te Raa GD, Pascutti MF, García-Vallejo JJ, et al. CMV-specific CD8⁺ T-cell function is not impaired in chronic lymphocytic leukemia. *Blood*. 2014;123(5):717-724.
- Jitschin R, Braun M, Büttner M, et al. CLL-cells induce IDOhi CD14+HLA-DRlo myeloid-derived suppressor cells that inhibit T-cell responses and promote TRegs. *Blood*. 2014;124(5):750-760.
- Bichi R, Shinton SA, Martin ES, et al. Human chronic lymphocytic leukemia modeled in mouse by targeted TCL1 expression. *Proc Natl Acad Sci USA*. 2002;99(10):6955-6960.
- Gorgun G, Ramsay AG, Holderried TAW, et al. E(μ)-TCL1 mice represent a model for immunotherapeutic reversal of chronic lymphocytic leukemia-induced T-cell dysfunction. *Proc Natl Acad Sci USA*. 2009;106(15):6250-6255.
- Hofbauer JP, Heyder C, Denk U, et al. Development of CLL in the TCL1 transgenic mouse model is associated with severe skewing of the T-cell compartment homologous to human CLL. *Leukemia*. 2011;25(9):1452-1458.
- McDermott DF, Atkins MB. PD-1 as a potential target in cancer therapy. *Cancer Med*. 2013;2(5):662-673.
- Ansell SM, Lesokhin AM, Borrello I, et al. PD-1 blockade with nivolumab in relapsed or refractory Hodgkin's lymphoma. *N Engl J Med*. 2015;372(4):311-319.
- Zhang L, Gajewski TF, Kline J. PD-1/PD-L1 interactions inhibit antitumor immune responses in a murine acute myeloid leukemia model. *Blood*. 2009;114(8):1545-1552.
- Sakuishi K, Apetoh L, Sullivan JM, Blazar BR, Kuchroo VK, Anderson AC. Targeting Tim-3 and PD-1 pathways to reverse T cell exhaustion and restore anti-tumor immunity. *J Exp Med*. 2010;207(10):2187-2194.
- Deng L, Liang H, Burnette B, et al. Irradiation and anti-PD-L1 treatment synergistically promote antitumor immunity in mice. *J Clin Invest*. 2014;124(2):687-695.
- Paterson AM, Brown KE, Keir ME, et al. The programmed death-1 ligand 1:B7-1 pathway restrains diabetogenic effector T cells in vivo. *J Immunol*. 2011;187(3):1097-1105.
- Burger JA, Tsukada N, Burger M, Zvaifler NJ, Dell'Aquila M, Kippes TJ. Blood-derived nurse-like cells protect chronic lymphocytic leukemia B cells

- from spontaneous apoptosis through stromal cell-derived factor-1. *Blood*. 2000;96(8):2655-2663.
24. Swirski FK, Nahrendorf M, Etzrodt M, et al. Identification of splenic reservoir monocytes and their deployment to inflammatory sites. *Science*. 2009;325(5940):612-616.
 25. Maffei R, Bulgarelli J, Fiorcari S, et al. The monocytic population in chronic lymphocytic leukemia shows altered composition and deregulation of genes involved in phagocytosis and inflammation. *Haematologica*. 2013;98(7):1115-1123.
 26. Ziegler-Heitbrock L, Ancuta P, Crowe S, et al. Nomenclature of monocytes and dendritic cells in blood. *Blood*. 2010;116(16):e74-e80.
 27. Yrlid U, Jenkins CD, MacPherson GG. Relationships between distinct blood monocyte subsets and migrating intestinal lymph dendritic cells in vivo under steady-state conditions. *J Immunol*. 2006;176(7):4155-4162.
 28. Arnold L, Henry A, Poron F, et al. Inflammatory monocytes recruited after skeletal muscle injury switch into antiinflammatory macrophages to support myogenesis. *J Exp Med*. 2007;204(5):1057-1069.
 29. Herishanu Y, Katz B-Z, Lipsky A, Wiestner A. Biology of chronic lymphocytic leukemia in different microenvironments: clinical and therapeutic implications. *Hematol Oncol Clin North Am*. 2013;27(2):173-206.
 30. Loke P, Allison JP. PD-L1 and PD-L2 are differentially regulated by Th1 and Th2 cells. *Proc Natl Acad Sci U S A*. 2003;100(9):5336-5341.
 31. Wintterle S, Schreiner B, Mitsdoerffer M, et al. Expression of the B7-related molecule B7-H1 by glioma cells: a potential mechanism of immune paralysis. *Cancer Res*. 2003;63(21):7462-7467.
 32. Chen L, Zhang Z, Chen W, et al. B7-H1 up-regulation on myeloid dendritic cells significantly suppresses T cell immune function in patients with chronic hepatitis B. *J Immunol*. 2007;178(10):6634-6641.
 33. Görgün G, Holderried TAW, Zahrieh D, Neuberg D, Gribben JG. Chronic lymphocytic leukemia cells induce changes in gene expression of CD4 and CD8 T cells. *J Clin Invest*. 2005;115(7):1797-1805.
 34. Curiel TJ, Wei S, Dong H, et al. Blockade of B7-H1 improves myeloid dendritic cell-mediated antitumor immunity. *Nat Med*. 2003;9(5):562-567.
 35. Wilcox RA, Feldman AL, Wada DA, et al. B7-H1 (PD-L1, CD274) suppresses host immunity in T-cell lymphoproliferative disorders. *Blood*. 2009;114(10):2149-2158.
 36. Spranger S, Koblisch HK, Horton B, Scherle PA, Newton R, Gajewski TF. Mechanism of tumor rejection with doublets of CTLA-4, PD-1/PD-L1, or IDO blockade involves restored IL-2 production and proliferation of CD8(+) T cells directly within the tumor microenvironment. *J Immunother Cancer*. 2014;2(1):3.
 37. Yu P, Steel JC, Zhang M, et al. Simultaneous inhibition of two regulatory T-cell subsets enhanced Interleukin-15 efficacy in a prostate tumor model. *Proc Natl Acad Sci USA*. 2012;109(16):6187-6192.
 38. Wainwright DA, Chang AL, Dey M, et al. Durable therapeutic efficacy utilizing combinatorial blockade against IDO, CTLA-4, and PD-L1 in mice with brain tumors. *Clin Cancer Res*. 2014;20(20):5290-5301.
 39. Motz GT, Coukos G. Deciphering and reversing tumor immune suppression. *Immunity*. 2013;39(1):61-73.
 40. Berger R, Rotem-Yehudar R, Slama G, et al. Phase I safety and pharmacokinetic study of CT-011, a humanized antibody interacting with PD-1, in patients with advanced hematologic malignancies. *Clin Cancer Res*. 2008;14(10):3044-3051.
 41. Westin JR, Chu F, Zhang M, et al. Safety and activity of PD1 blockade by pidilizumab in combination with rituximab in patients with relapsed follicular lymphoma: a single group, open-label, phase 2 trial. *Lancet Oncol*. 2014;15(1):69-77.